JOURNAL OF BACTERIOLOGY, May 2011, p. 2197–2207 Vol. 193, No. 9
0021-9193/11/$12.00 doi:10.1128/JB.01450-10

Transcriptional Regulation of the Gene Cluster Encoding Allantoinase and Guanine Deaminase in *Klebsiella pneumoniae*▽

Karla Guzmán, Josefa Badia, Rosa Giménez, Juan Aguilar,* and Laura Baldoma

Departament de Bioquímica i Biología Molecular, Institut de Biomedicina de la Universitat de Barcelona, Facultat de Farmacia, Universitat de Barcelona, E-08028 Barcelona, Spain

Received 30 November 2010/Accepted 17 February 2011

Purines can be used as the sole source of nitrogen by several strains of *K. pneumoniae* under aerobic conditions. The genes responsible for the assimilation of purine nitrogens are distributed in three separated clusters in the *K. pneumoniae* genome. Here, we characterize the cluster encompassing genes KPN_01787 to KPN_01791, which is involved in the conversion of allantoin into allantoate and in the deamination of guanine to xanthine. These genes are organized in three transcriptional units, *hpxSAB*, *hpxC*, and *guaD*. Gene *hpxS* encodes a regulatory protein of the GntR family that mediates regulation of this system by growth on allantoin. Proteins encoded by *hpxB* and *guaD* display allantoinase and guanine deaminase activity, respectively. In this cluster, *hpxSAB* is the most tightly regulated unit. This operon was activated by growth on allantoin as a nitrogen source; however, addition of allantoin to nitrogen excess cultures did not result in *hpxSAB* induction. Neither *guaD* nor *hpxC* was induced by allantoin. Expression of *guaD* is mainly regulated by nitrogen availability through the action of NtrC. Full induction of *hpxSAB* by allantoin requires both HpxS and NAC. HpxS may have a dual role, acting as a repressor in the absence of allantoin and as an activator in its presence. HpxS binds to tandem sites, S1 and S2, overlapping the −10 and −35 sequences of the *hpxSAB* promoter, respectively. The NAC binding site is located between S1 and S2 and partially overlaps S2. In the presence of allantoin, interplay between NAC and HpxS is proposed.

Purines are nitrogen-rich compounds that are widespread in the biosphere. When ammonia, the preferred nitrogen source, is limiting, many microorganisms can obtain nitrogen from purines. The first step in the assimilation of adenine or guanine as a nitrogen source is a deamination reaction catalyzed by specific enzymes, yielding one molecule of ammonia and one molecule of hypoxanthine or xanthine, respectively. The catabolic pathway for hypoxanthine and xanthine assimilation occurs in two stages. In the first stage, both compounds are oxidized by the action of xanthine dehydrogenase to uric acid, which is then converted to allantoate via allantoin by two sequential ring-opening steps (Fig. 1A). In the second stage, allantoate is transformed to CO_2 plus ammonia. Although the first part of this pathway is common to all species studied so far, the degradation of allantoate can follow different routes depending on the microbial species (8, 28, 42, 43, 44).

Among enterobacteria, purine catabolism has been characterized for *Escherichia coli* and some species of *Klebsiella*. In *E. coli*, nitrogen assimilation from adenine is incomplete, since allantoin is not further metabolized in the presence of oxygen (43). Nitrogen assimilation from allantoin involves allantoate amidohydrolase and ureidoglycolate dehydrogenase, enzymes encoded by genes of the *all* regulon, whose expression takes place only under anaerobic conditions in *E. coli* (8, 32). In contrast, in *Klebsiella*, the purine catabolic pathway is complete and proceeds past allantoin since all nitrogens are assimilated under aerobic conditions (10, 28).

In *Klebsiella pneumoniae* strain KC2653, the *hpx* genetic system responsible for the oxidation of hypoxanthine to allantoin has been characterized by de la Riva et al. (10). This cluster of seven genes is organized in four transcriptional units, *hpxDE*, *hpxR*, *hpxO*, and *hpxPQT*. Gene *hpxP* encodes hypoxanthine permease; genes *hpxDE* encode the enzyme involved in the oxidation of hypoxanthine to uric acid, which is a two-component oxygenase structurally related to the class of IB dioxygenases described by Batie et al. (3) involved in aromatic ring hydroxylations; gene *hpxO* encodes an FAD-dependent monooxygenase involved in the oxidation of uric acid to 5′-hydroxyisourate (HIU) that has been characterized by O'Leary et al. (27); and gene *hpxT* encodes the HIU hydrolase involved in the transformation of HIU to 2-oxo-4-hydroxy-4-carboxy-5-ureidoimidazoline (OHCU). The latter compound undergoes stereoselective decarboxylation to produce CO_2 and *S*-allantoin by the action of OHCU decarboxylase, encoded by gene *hpxQ*. Expression of this system is activated by nitrogen limitation and by the presence of specific substrates, with *hpxDE* and *hpxPQT* controlled by both signals. Induction of *hpxPQT* requires uric acid formation, whereas expression of *hpxDE* is induced by the presence of hypoxanthine through the HpxR regulatory protein, encoded by the *hpxR* gene (10).

The metabolism of purines has also been studied by Pope et al. (28) for *Klebsiella oxytoca* M5a1. In this strain, a cluster of 23 genes responsible for the utilization of purines as the sole nitrogen source has been identified. The function of some genes of this cluster was assigned by growth, complementation tests, and sequence similarity. Comparison with the *K. pneumoniae* MGH78578 genome revealed that these genes are organized in three separated clusters in *K. pneumoniae*. Genes KPN_01787 to KPN_01790 have been proposed to be involved

* Corresponding author. Mailing address: Departament de Bioquímica i Biologia Molecular, Facultat de Farmàcia, Universitat de Barcelona, Av. Diagonal, 643, E-08028 Barcelona, Spain. Phone: 34-934034496. Fax: 34-934024520. E-mail: juanaguilar@ub.edu.

▽ Published ahead of print on 25 February 2011.

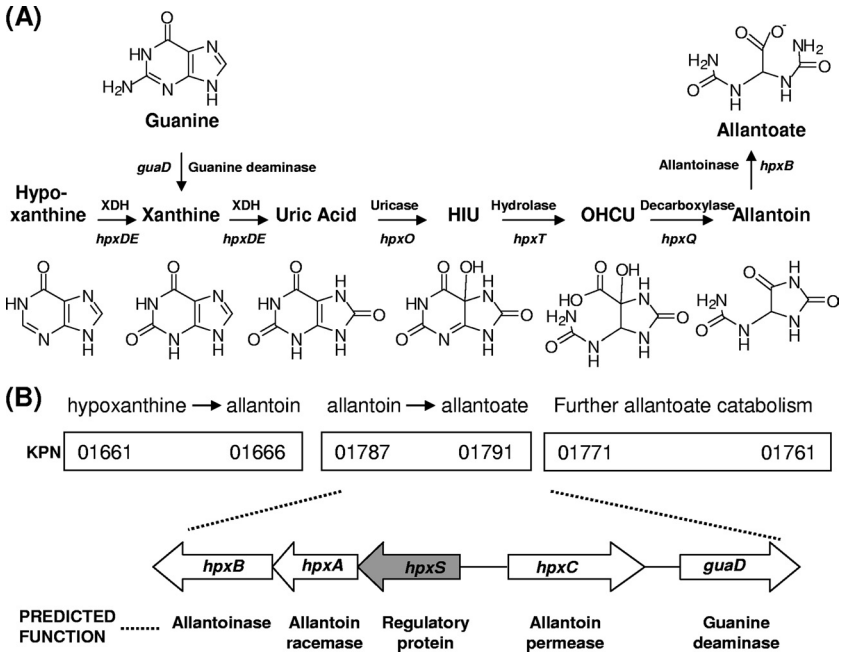

FIG. 1. (A) Metabolic map for guanine and hypoxanthine assimilation to allantoate. For each enzymatic step, the associated gene in *K. pneumoniae* is indicated. (B) Gene organization of the three clusters involved in the assimilation of purine nitrogens in *K. pneumoniae* as described by Pope et al. (28). A more detailed scheme of the gene organization of the cluster studied in this work is presented below. The arrows show the extents and directions of transcription of the genes. The predicted function of the *hpx*-encoded proteins is indicated below each gene. XDH, xanthine dehydrogenase; HIU, 5-hydroxyisourate; OHCU, 2-oxo-4-hydroxy-4-carboxy-5-ureidoimidazoline.

in the metabolism of allantoin to allantoate, and gene KPN_01791 has been proposed to be involved in guanine deamination (Fig. 1B).

In the presence of ammonia, there is a strong repression of many systems that allow enterobacterial species such as *E. coli* or *K. pneumoniae* to use alternative nitrogen sources such as amino acids or purines. When ammonia is limiting, the ability of cells to obtain nitrogen from these compounds usually requires a two-component system in which phosphorylated NtrC binds to an enhancer and interacts with RNA polymerase bearing the sigma factor σ^{54}. The Ntr (nitrogen-regulated) system activates a set of genes involved in the catabolism of nitrogenous compounds whose degradation products include ammonia or glutamate (30). The Ntr system also activates the transcription of the nitrogen assimilation control protein (NAC) that regulates a subset of genes that are dependent on RNA polymerase bearing σ^{70} for their transcription (11, 18, 24, 38). Thus, NAC couples the σ^{54}-dependent transcription of the Ntr system with that of the σ^{70}-dependent catabolic genes. Recently, more than 90 new NAC target genes have been identified by chromatin immunoprecipitation experiments with *K. pneumoniae.* The KPN_01789/01790 intergenic region was among the promoter sequences that were coimmunoprecipitated with NAC (13).

In this study, we characterize the KPN_01787/01791 gene cluster of *K. pneumoniae* KC2563, which contains the genes responsible for allantoin-to-allantoate metabolism and gene *guaD*, involved in the deamination of guanine to xanthine. Regulation analysis of the different transcriptional units by nitrogen limitation or by the HpxS-specific regulator is approached. In addition, evidence for the catalytic activity of GuaD as guanine deaminase and HpxB as allantoinase is provided.

MATERIALS AND METHODS

Bacterial strains and plasmids. The genotypes and sources of the bacterial strains, plasmids, and promoter fusions are given in Table 1. All *K. pneumoniae* strains are derived from strain W70 (25). Genetic crosses were performed by P1-mediated transduction (15).

Growth conditions and preparation of cell extracts. Cultures were grown at 30°C with aeration in Luria broth (LB) (7) or in W4 minimal medium (41) supplemented with glucose at 0.4% as the sole carbon source. NaCl was removed from LB plaques for selection of directed mutants. For limiting-nitrogen conditions, freshly made glutamine (Gln) was used at 0.04%. Ammonium sulfate and Gln (NGln), both at 0.2%, were used for nitrogen excess (4, 5). Hypoxanthine and uric acid were prepared as described by Rouf and Lomprey (34). Allantoin, allantoate, guanosine, and adenosine were used at 0.05%. The selection medium in the conjugation experiments consisted of W4 minimal medium supplemented with sodium citrate at 0.4% as the carbon source and ammonium sulfate at 0.2% as the nitrogen source, supplemented with the appropriate antibiotics. When required, the following antibiotics were used at the indicated concentrations: ampicillin (Ap), 100 μg/ml; kanamycin (Km), 50 μg/ml; streptomycin (Sm), 50 μg/ml; and tetracycline (Tet), 30 μg/ml. 5-Bromo-4chloro-3-indolyl β-D-galactoside (X-Gal), and isopropyl-β-D-thiogalactoside (IPTG) were used at 30 and 10 μg/ml, respectively.

Cell extracts were obtained by sonic disruption of bacterial cells collected by centrifugation at the end of the exponential phase and resuspended in the appropriate buffer.

Enzyme activities. For β-galactosidase activity, cultures were grown to an optical density at 600 nm (OD_{600}) of 0.5. Cells were collected by centrifugation, washed in 1% KCl, and suspended at a concentration that involved 1 to 1.5 mg of protein per ml (2). β-Galactosidase activity was assayed in detergent-treated whole cells, using *o*-nitrophenyl-β-D-galactopyranoside (ONPG) as the substrate, and was expressed in U/mg of cell protein (26). One unit of β-galactosidase activity corresponds to the amount of enzyme that hydrolyzes 1 nmol of ONPG

TABLE 1. Strains and plasmids used in this study

Strain, fusion, or plasmid	Relevant characteristic(s)	Source or reference
K. pneumoniae strains		
KC2653	*hutC515* Δ[*bla*]-*2 dadA1 str-6*	22
KC5249	*hutC515* Δ[*bla*]-*2 nac-2*	R. A. Bender
KC2738	*hutC515 ntrC*::Tn*5-131*	6
KB17K	KC2653 *hpxS*::*kan*	This study
E. coli strains		
XL1-Blue	*recA1 endA1 gyrA96 thi-1 hsdR17 supE44 relA1 lac* [F′ *proAB lacI*^{q}ZΔM15 Tn*10*(Tc^r)]	Stratagene
S17(λ pir)	Tp^r Sm^r *recA thi pro hsdR hsdM*$^+$ RP4::2-Tc::Mu::Km Tn*7* λ	Biomedal
EB6193	RP4-2 *tet* Mu-1 Kan::Tn*7* integrant; *leu-63*::IS*10 recA1 creC510 hsdR17 endA1 zbf-5 uidA*(ΔMuI)::*pir*$^+$ *thi* Sp^r Sm^r	R. A. Bender
DH5αF′	ϕ80d*lacZ*ΔM15 *recA1 endA1* λ$^-$ *gyrA96 thi-1 hsdR17* (r_K^- m_K^+) *phoA supE44 relA1 deoR* Δ(*lacZYA-argF*)*U169*	Gibco BRL
EB4335	DH5α/pCB1083; pCB1026	33
Fusions[a]		
Φ(*hpxS-lacZ)*	*hpxS* (positions −263 to +92) fused to *lacZ*	This study
Φ(*hpxC-lacZ)*	*hpxC* (positions −189 to +170) fused to *lacZ*	This study
Φ(*guaD-lacZ)*	*guaD* (positions −156 to +83) fused to *lacZ*	This study
Plasmids		
pGEMT	Ap^r; cloning vector for PCR products	Promega
pKAS32	Ap^r; pGP704; *rpsL*	40
pRS415	Ap^r; promoterless *lacZYA* reporter for operon fusions	39
pCB1583	Ap^r Km^r; promoterless *lacZ* reporter for integration of operon fusions into host genome with *oriR6K* replication origin; *rpsL*	R. A. Bender
pMAL-c2x	Ap^r; vector for cytoplasmic expression of maltose binding protein fusions	New England Biolabs
pKD4	Ap^r Km^r	9
pCB1083	*lacI*^{q} cloned into pACYC184	33
pCB1026	Wild-type *nac* cloned in pQE70	33

[a] Nucleotide sequences are given in the 5′-to-3′ direction for the coding strand of each gene and are numbered relative to the gene transcription initiation nucleotide at position +1.

per min. The data reported are the averages from at least four separate experiments performed in triplicate.

Allantoinase was assayed as described previously (8). The assay was based on the colorimetric method described by Lee and Roush (21) applied to the reaction of the allantoate product with phenylhydrazine-HCl and potassium ferricyanide.

Guanine deaminase was determined as described elsewhere (35). Assays were performed with a final volume of 1 ml containing 20 mM potassium phosphate buffer (pH 7.4), 60 μM guanine, and 0.01 U commercial xanthine oxidase (Sigma-Aldrich, Germany). Uric acid produced in the reaction was monitored by its specific absorbance at 293 nm (ε = 12 mM/cm). For kinetic parameter determination, guanine concentrations ranging from 5 to 250 μM were used.

Protein concentration was determined by the method of Lowry et al. (23), with bovine serum as a standard.

DNA manipulation and site-directed mutagenesis. Bacterial genomic DNA was obtained using a Wizard genomic DNA purification kit (Promega), and plasmid DNA was prepared using the Wizard Plus SV Midipreps DNA purification system (Promega). DNA manipulations were performed essentially as described by Sambrook and Russell (36). DNA fragments were amplified by PCR, using chromosomal DNA as a template. When necessary, specific restriction sites were incorporated at the 5′ ends of the primers to facilitate the cloning of the fragments in the appropriate vector. PCRs were performed with *Pfu* DNA polymerase under standard conditions. DNA was sequenced using an automated ABI 377 DNA sequencer and fluorescent-dye termination methods.

Site-directed mutagenesis of HpxS or NAC binding sites was performed by PCR using primers containing the desired mutations. All primers used are listed in Table 2.

Mapping of the 5′ end of the *hpxC*, *hpxSAB*, and *guaD* transcripts. The 5′ regions of the *hpxC*, *hpxSAB*, and *guaD* transcripts were determined by rapid amplification of cDNA 5′ ends (5′-RACE) (36) using a commercial 5′-RACE kit (Roche Diagnostics, GmbH). Total RNA was isolated from KC2653 cells grown aerobically to an OD_{600} between 0.5 and 1 in glucose minimal medium with glutamine at 0.04% as a nitrogen source (nitrogen-limiting conditions) using a Qiagen RNeasy total RNA kit and then treated with RNase-free DNase (Ambion). For mapping the 5′ end of *hpxSAB*, RNA was also obtained from cells grown in glucose minimal medium with allantoin as the sole nitrogen source. The cDNAs were transcribed from RNA with specific *hpxC*, *hpxSAB*, or *guaD* antisense oligonucleotides. A homopolymeric (dA) tail was added (via terminal transferase) to the 3′ termini of the corresponding cDNAs. Amplification of reverse transcription products was performed with nested gene-specific primers and an oligo(dT) anchor primer. The double-stranded cDNAs obtained were cloned into pGEMT vector for sequencing.

Directed mutagenesis of the *K. pneumoniae hpxS* gene. An *hpxS* knockout mutant of *K. pneumoniae* KC2653 was generated by antibiotic marker exchange using the suicide plasmid pKAS32. This vector contains the R6K origin of replication, which functions only in bacteria that produce the replication protein π. In addition, this vector expresses the *E. coli rpsL* gene, encoding ribosomal protein S12, which provides a positive selection for bacteria that have exchanged cloned plasmid sequences with the corresponding chromosomal sequences.

To clone the *hpxS* gene, primers were designed to amplify the corresponding open reading frames plus their flanking regions by PCR. A Km cassette was obtained by inserting the Km resistance gene *kan*, which was obtained by PCR amplification from plasmid pKD4 (9), into the corresponding coding region. In the Km cassette, the *kan* gene was flanked by *K. pneumoniae*-specific genomic sequences of at least 500 bp. Mutagenesis of the chromosomal gene was carried out by homologous recombination between the Km cassette and the wild-type gene after *E. coli* S17.1 (λ pir) harboring the recombinant pKAS32 derivative containing the Km cassette was mated with *K. pneumoniae* KC2653 as the recipient.

To construct the *hpxS* knockout mutant, the Km cassette was obtained as follows. A 1,787-bp fragment encompassing *hpxS* and its flanking regions was amplified by PCR from genomic DNA of strain KC2653. Restriction sites for EcoRV or EcoRI were incorporated at the 5′ ends of the primers to facilitate directed cloning of the amplified fragment into pKAS32. Disruption of the

TABLE 2. Oligonucleotides used in this study

Primer	Sequence[a]	Experiment
Psc(1)_EcoRI.fw	CG**GAATTC**TGGTAAATGCTTT	Construction of Φ(*hpxC-lacZ*)
Psc(1)_Sma1.rv	TCC**CCCGGG**TGTGCACGTCCGAC	
Psc(2)_EcoRI.fw	CG**GAATTC**TGTGCACGTCC	Construction of Φ(*hpxSAB-lacZ*)
Psc(2)_Sma1.rv	TCC**CCCGGG**TGGTAAATGCTTTC	
PguaD_EcoRI.fw	CG**GAATTC**CCACCTACCGC	Construction of Φ(*guaD-lacZ*)
PguaD_BamHI.rv	CGC**GGATCC**ACGCCGGCGATA	
HpxS_BamHI.rv	CG**GGATCC**TCACGACTCCTT	Cloning of *hpxS* in pMAL-c2x
HpxS_EcoRI.fw	CG**GAATTC**ATGAATAATGAACATCGTCTCCAGG	
PmalregguaD1.fw	CGC**GAATTC**ATGATGGATTACCAGACCGC	Cloning of *guaD* in pMAL-c2x
pmalguaD.rv	AAT**TCTAGA**TCAATCCTGACACCACACCCGCTC	
pmalregpuuE1.fw	CGC**GAATTC**ATGGGAGAGAACCAGGAACAC	Cloning of *hpxB* in pMAL-c2x
pmalpuuE.rv	AAT**TCTAGA**CTACCCGCGATACGGATGGGTTTCG	
hpxC_sp1	GAACCTGCCAGCTGGCCAGC	Mapping of the 5′ end of the *hpxC* transcript
hpxC_sp3	TGGTCGCGGGTCGGCGCCAG	
hpxS_sp1	TGACCAGTTGCACAGCGGCG	Mapping of the 5′ end of the *hpxSAB* transcript
hpxS_sp2	CGGCTCACGGCGAACACCTC	
hpxS_sp3	CGATAGCCGTCATCAGCGCC	
guaD_sp1	GATCGACATAGCCCTTCAGG	Mapping of the 5′ end of the *guaD* transcript
guaD_sp2	AGCAGGGCGATAATTTTCCC	
guaD_sp3	CCTCATCCGGGGTCTCCGCC	
HpxSmut2	GCC**GAATTC**GACCATCGTCGCCATATGCATTGC	Directed mutagenesis of the *hpxS* gene
HpxSmut1_EcoRI	AAACCGCCGGACCAGC**GAATTC**CGG	
KanXho.fw	GACATA**CTCGAG**GTGTAGGCTGGAGCTGCTTC	Directed mutagenesis of the *hpxS* gene
KanXho.rv	AGTATC**CTCGAG**CATATGAATATCCTCCTTAG	
Psc(2)_Sma1.rv	TCC**CCCGGG**TGGTAAATGCTTTC	Probe P1
Psc(2)_del1.rv	TCCTCTGAATGAAAACCCTTTG	
Psc(2)_Sma1.rv	TCC**CCCGGG**TGGTAAATGCTTTC	Probe P2
Psc(2)_del2.rv	GAATGATGAATCTTGTATAC	
Psc(2)_Sma1.rv	TCC**CCCGGG**TGGTAAATGCTTTC	Probe P4
Psc(2)_del3.rv	GATCTGCTATCGATAAGTG	
Psc(1)_Sma1.rv	TCC**CCCGGG**TGTGCACGTCCGAC	Probe P6
Psc(1)_del1.fw	GGTTTCACTTATCGATAGCAG	
Psc(1)_Sma1.rv	TCC**CCCGGG**TGTGCACGTCCGAC	Probe P7
Psc(1)_del2.fw	GTATACAAGATTCATCATTC	
Psc(1)_Sma1.rv	TCC**CCCGGG**TGTGCACGTCCGAC	Probe P8
Psc(1)_del3.fw	GCCTCAGCAATCCATATCAAAGG	
Psc(1)_EcoR1.fw	CG**GAATTC**TGGTAAATGCTTT	Probe P3
ShpxS1.rv	TTAAATTTTATGTATACGATCTGCTATCG	
Psc(1)_EcoR1.fw	CG**GAATTC**TGGTAAATGCTTT	Probe P3* (mutated S1)
ShpxSmut1.rv	TTAAATTTTATTCATGGGATCTGCTATCGATAAGTG	
ShpxS2.fw	ATTTAATTTTTGTATACAAGATTCATCATTCTGGC	Probe P5
Psc(2)_del1.rv	TCCTCTGAATGAAAACCCTTTG	
ShpxSmut2.fw	ATTTAATTTTTCCATGAAAGATTCATCATTCTGGC	Probe P5* (mutated S2)
Psc(2)_del1.rv	TCCTCTGAATGAAAACCCTTTG	
NACboxmut.fw	CGATAGCAGATCGTATACATAAAGGCATAATTTTTGGCAACAAGA	Probe m-NAC site
NACboxmut.rv	CCAGGCCAGAATGATGAATCTTGTTGCCAAAAATTATGCTTTATG	

[a] Restriction sites incorporated at the 5′ end are in bold. Nucleotides changed to obtain mutated probes are underlined.

cloned *hpxS* gene was performed by insertion of the *kan* gene into the XhoI site located 291 bp downstream of the ATG codon.

The obtained pKAS32 recombinant plasmid was propagated into strain EB6193 and introduced into *E. coli* S17.1(λ pir) for mating with the recipient Sm^r strain KC2653 as described previously. Transconjugants were selected for resistance to Km on citrate plates and further purified in this medium. Isolated colonies were then grown on LB plates without NaCl containing Km and Sm (1 mg/ml) to facilitate homologous recombination. After several rounds of growth at 30°C in this medium, colonies were screened for sensitivity to Ap in order to identify which transconjugants had undergone allelic exchange and therefore did not carry the plasmid integrated (merodiploids of the target gene). Gene disruption of the correct target gene was verified by PCR and subsequent sequencing. In this way, strain KB17K was selected for further studies.

Construction of *lacZ* transcriptional fusions. Transcriptional fusions were constructed by inserting the promoter fragments into plasmid pRS415 (39). This plasmid carries a cryptic *lacZ* operon and confers resistance to ampicillin. To construct the *hpxSAB-lacZ* fusion, a 360-bp fragment encompassing the *hpxSAB-hpxC* intergenic region was amplified by PCR, cloned into plasmid pRS415 using the EcoRI-BamHI sites. The same promoter fragment was cloned in the opposite direction to construct the *hpxC-lacZ* fusion. For all constructs, plasmid DNA was sequenced to ensure that that fragment was inserted in the correct orientation and that no mutations had been introduced during the amplification reaction.

To transfer the *lacZ* fusions into *K. pneumoniae* chromosome as a single copy, the recombinant plasmid was first digested with EcoRI and SacI, and the fragment containing the promoter fusion was subcloned into plasmid pCB1583 (22). This is a λ *pir*-dependent plasmid whose *lacZ* gene is flanked by genes of the *K. pneumoniae* D-ribose operon, thus allowing the integration of the cloned fusion by homologous recombination into the D-ribose operon of the *K. pneumoniae* recipient strain. The recombinant plasmids containing Φ(*hpxSAB-lacZ*) or Φ(*hpxC-lacZ*) were selected after transformation of strain EB6193 as blue colonies on LB–X-Gal–Km plates and then introduced into *E. coli* S17.1(λ *pir*) by electroporation. After several rounds of selection in different growth media, stable recombinants in the *rbs* locus were isolated as those displaying a Km^s Sm^r D-ribose-negative phenotype. To transfer the fusions in the *K. pneumoniae* chro-

mosome, conjugation was performed with the double-rifampin-streptomycin-resistant derivative of *K. pneumoniae* strain KC2653. After several rounds of selection in different growth media, stable recombinants were isolated as those displaying a Km^s Sm^r D-ribose negative phenotype.

Expression and purification of recombinant proteins. GuaD, HpxB, and HpxS were purified using the *malE* gene fusion system. For this purpose, the corresponding genes (*guaD*, *hpxB*, and *hpxS*) were amplified by PCR and cloned into the plasmid pMal-c2x. The restriction sites used for *hpxS* cloning were BamHI and EcoRI, whereas those used for *guaD* and *hpxB* cloning were EcoRI and XbaI. In all cases, the forward primer was designed to fuse the ATG start codon of each gene in-frame with *malE*. Overproduction of MalE-fused proteins was achieved in strain XL1-Blue carrying the recombinant plasmid. The induction conditions were 0.5 mM IPTG for 16 h at 30°C for MalE-HpxS and 0.3 mM IPTG for 3 h at 37°C for MalE-GuaD and MalE-HpxB. The fusion proteins were then purified by affinity chromatography with amylose resin (New England BioLabs) in accordance with the manufacturer's instructions. For protein purification, the cell pellet from 100 ml culture of strain XL1-Blue bearing the recombinant plasmid was suspended in 2 ml of column buffer (20 mM Tris-HCl, pH 7.4, containing 0.2 M NaCl and 1 mM EDTA) and sonicated on ice. The cell lysate was centrifuged at 15,000 × *g*, and the supernatant was loaded onto the amylose resin column. After the mixture was loaded onto the column, the resin was washed with column buffer. Elution was performed with column buffer containing 10 mM maltose, and the fusion protein was digested with factor Xa by incubation at room temperature for 12 h. The cleaved HpxS protein was used in gel shift experiments. However, MalE-HpxB and MalE-GuaD folding made difficult the cleavage of the fusion protein in solution (digestion was less than 50%). Recombinant MalE-HpxB and MalE-GuaD were used in enzyme activity assays since no changes in activity were observed for these fused proteins with respect to HpxB or GuaD obtained after cleavage of the recombinant MalE-fused proteins inside the amylose column.

His-tagged NAC was purified using nickel affinity resin as described elsewhere (33). One-liter cultures (LB supplemented with 100 μg/ml of ampicillin and 10 μg/ml of tetracycline) of strain EB4335 harboring plasmids pCB1083 and pCB1026 were grown to an OD_{600} of 0.6. At this point, IPTG was added to give a concentration of 1 mM to induce the production of the protein. After 4 h of incubation, the cell pellet was suspended in 5 ml of column buffer (100 mM sodium phosphate [pH 7.0], 250 mM NaCl, 2.5 mM $MgCl_2$, 10% glycerol, 10 mM imidazole, and 1 mM 2-mercaptoethanol) and sonicated on ice. The cell lysate was centrifuged at 15,000 × *g*, and the supernatant was incubated with 1 ml of nickel resin with agitation for 1 h at 4°C. This mixture was poured to a column, and the resin was first washed with 20 to 30 ml of wash buffer (100 mM sodium phosphate [pH 7.0], 500 mM NaCl, 2.5 mM $MgCl_2$, 10% glycerol, 90 mM imidazole, and 1 mM 2-mercaptoethanol). Elution was performed with column buffer containing 250 mM imidazole. Fractions were pooled and dialyzed overnight to remove imidazole.

Purified proteins were analyzed by sodium dodecyl sulfate-polyacrylamide gel electrophoresis (SDS-PAGE) performed according to the standard procedure (19) and were either used immediately or stored at −20°C in glycerol to 20%.

DNA binding studies. The nonradioactive digoxigenin (DIG) gel shift kit for 3′-end labeling of DNA fragments (Roche Applied Science, Indianapolis, IN) was used for protein-DNA binding assays. The fragments obtained by PCR were labeled with terminal transferase and digoxigenin-ddUTP according to the manufacturer's instructions (Roche).

Labeled DNA fragments were incubated either with purified HpxS or NAC in 10 mM Tris-HCl (pH 7.4), 100 mM KCl, 10 mM $MgCl_2$, 10% glycerol, and 2 mM dithiothreitol in a total volume of 20 μl. Poly(dI-dC) was used as a nonspecific competitor. When indicated, a 10-fold excess of noncompetitive or competitive nonlabeled DNA was added to the reaction mixtures. HpxS binding mixtures were incubated for 20 min at 37°C, whereas NAC binding mixtures were incubated at room temperature for 20 min (14) and then loaded onto a prerun gel of 5% native polyacrylamide, containing 10% glycerol in 1× TBE (Tris-borate-EDTA buffer). Blotting was performed using a Bio-Rad electroblotting system (model Trans blot) according to the manufacturer's instructions. Chemiluminescence detection of DIG-labeled DNA-protein complexes on the nylon membranes was detected using Hyperfilm ECL (Amersham Pharmacia).

RESULTS AND DISCUSSION

Transcriptional organization of the *hpxBASC-guaD* gene cluster. By similarity to *K. oxytoca*, the gene cluster encompassing genes KPN_01787 to KPN_01791 in *K. pneumoniae* has been proposed to encode allantoinase (*hpxB*), allantoin racemase (*hpxA*), a regulatory protein of the GntR familiy (*hpxS*), allantoin permease (*hpxC*), and guanine deaminase (*guaD*) (Fig. 1) (28). However, no experimental evidence for the transcriptional regulation of these genes is available.

An *in silico* analysis of the intergenic region between *hpxSAB* and *hpxC* and the *guaD* 5′-flanking region using the Footprint and Promscan programs (http://www.promscan.uklinux.nrt/home.html) identified a putative σ^{70} promoter at the 5′ end of *hpxSAB* and putative σ^{54} promoters at the 5′ ends of the *hpxC* and *guaD* genes. In addition, putative sites for NtrC were also visualized (Fig. 2), suggesting that the expression of these genes may be regulated by nitrogen availability.

The 5′ ends of the *hpxSAB*, *hpxC*, and *guaD* transcripts were experimentally determined by the 5′-RACE method (Fig. 2B). Total RNA was obtained from aerobic cultures of strain KC2653 on glucose-glutamine. For *hpxSAB*, the transcriptional start site was identified 26 nucleotides upstream of the ATG codon of the *hpxS* gene. The same 5′ end was identified in cells grown in the presence of allantoin. Inspection of the sequences upstream of nucleotide +1 revealed the presence of the −10 (TATACG) and −35 (TATACA) sequences, similar to the σ^{70} consensus sequence separated by 16 bp (positions matching the consensus are underlined) (Fig. 2A). For *guaD*, a sequence matching the consensus sequence reported for σ^{54} RNA polymerase was identified upstream of the corresponding nucleotide at position +1 (Fig. 2A). However, for *hpxC*, the putative σ^{54} recognition sequence identified *in silico* (CTGGCCTGGATCCTGCAA) was located between positions −20 and −3 with respect to the experimentally determined nucleotide at position +1. Therefore, this sequence does not fit the optimal location for σ^{54} promoters, and it is unlikely to be functional. Inspection of this region revealed the presence of the −10 (GATCCT) and −35 (TATACA) sequences, similar to the σ^{70} consensus sequences, which are separated by an unusually long stretch of 20 bp (Fig. 2A). Although this spacer does not fit the optimal 17 ± 1-bp length, spacers from 15 to 21 bp have been described (17). For σ^{70}-dependent *E. coli* promoters, the spacing of promoter elements can regulate the basal expression of the corresponding gene (16).

Thus, experimental identification of the transcriptional start sites confirmed the organization of this cluster in three transcriptional units. As expected, transcription of *guaD* depends on the σ^{54} RNA polymerase subunit whereas transcription of *hpxSAB* depends on σ^{70}. Regarding *hpxC*, our results suggest that its transcription may be driven by σ^{70} RNA polymerase.

The protein encoded by *guaD* displays guanine deaminase activity. Sequence analysis of *K. pneumoniae* GuaD using a BLAST search showed that this protein has 86% identity with the proposed guanine deaminase of *K. oxytoca* and 58% identity with *E. coli* GuaD. The sequence includes the motif PGF VDAHVH between positions 73 and 81, which matches the consensus sequence implicated in metal binding (Zn^{2+}) in prokaryotic proteins of the cyclic amidohydrolase family (12). This motif is also present in *K. oxytoca* GuaD (28).

To confirm GuaD function, the corresponding gene of strain KC2653 was cloned in plasmid pMal-c2X, and the protein was purified as described in Materials and Methods. The activity of the purified enzyme was determined using guanine or adenine as a substrate. The results showed only activity toward guanine.

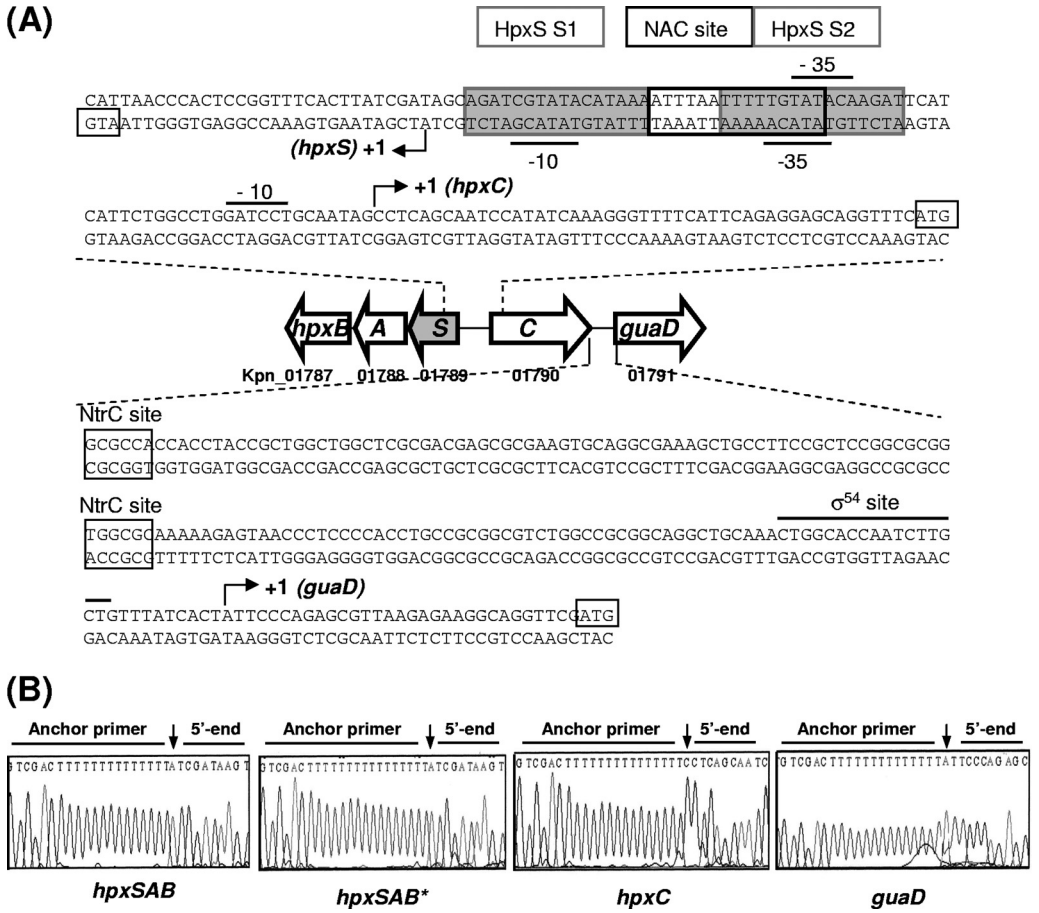

FIG. 2. (A) Promoter sequences of the *hpxBASC-guaD* gene cluster. For each gene, the ATG initiation codon is boxed, the consensus sequence for RNA polymerase (the −10 and −35 sequences for σ^{70} recognition in *hpxSAB* and *hpxC* or the σ^{54} recognition sequence in *guaD*) is indicated, and the transcriptional start site is shown by a black arrowhead labeled +1. Putative NtrC binding sites identified using the Promscan and Virtual Footprint programs are indicated. Proposed binding sites for NAC and HpxS (S1 and S2) are also indicated (sites were proposed according to EMSA results and similarity to the consensus sequence of each regulatory protein). (B) Identification of the 5′ ends of the indicated genes by sequencing across ligation sites of 5′-RACE products. Chromatograms display the sequences at ligation sites of typical cloned 5′-RACE products derived from transcripts obtained from strain KC2653 cells grown in low-ammonia medium (GGln). For *hpxSAB*, this analysis was also performed with cells grown in the presence of allantoin (*hpxSAB**). Arrows indicate the transcription initiation site.

The kinetic parameters for guanine were determined under standard reaction conditions (pH 7.4; 37°C) from the double-reciprocal Lineweaver-Burk plot. This analysis yielded a K_m value of 8.9 μM and a V_{max} value of 1.13 μmol min^{-1} mg^{-1}.

The protein encoded by *hpxB* displays allantoinase activity. The protein encoded by gene *hpxB* (KPN_ 01787) in *K. pneumoniae* displayed 89% identity with HpxB of *K. oxytoca* (28) and 58% identity with the metal-independent allantoinase encoded by *puuE* in *Pseudomonas fluorescens* (29). In *K. oxytoca*, the ortholog *hpxB* gene was proposed to encode allantoinase since *hpxB* insertion mutants failed to grow with allantoin as the sole nitrogen source but displayed normal growth with allantoate (28).

To confirm HpxB function in *K. pneumoniae*, the gene *hpxB* of strain KC2653 was cloned in plasmid pMal-c2X, and the protein was purified. The activity of the purified enzyme was determined using allantoin as a substrate, as described in Materials and Methods. The specific enzyme activity was 390 U/mg. Purified HpxB displayed allantoinase activity in the absence of any bivalent metal.

HpxB does not display similarity to metal-dependent allantoinases belonging to the amidohydrolase superfamily (20). Instead, this protein displays high similarity to PuuE, a novel allantoinase of *Pseudomonas fluorescens* that is annotated in structure and sequence databases as polysaccharide deacetylase on the basis of its similarity to enzymes that remove N-linked or O-linked acetyl groups from cell wall polysaccharides (29). As for HpxB, other enzymes of the purine catabolic pathway encoded in *K. pneumoniae*, such as xanthine oxidase (*hpxDE*) and uricase (*hpxO*), do not display similarity to other reported enzymes known to catalyze these reactions (10). The lack of similarity to proteins with equivalent activity in other bacteria seems to be a general feature for enzymes of the purine assimilation pathway in *K. pneumoniae*. This finding, together with the distribution of these genes in separate clusters, suggests that the purine assimilation pathway in *K. pneumoniae* may have an evolutionary origin different from that of other enterobacteriaceae.

Since allantoinases such as PuuE display stereospecificity for the S enantiomer of allantoin and the product generated by

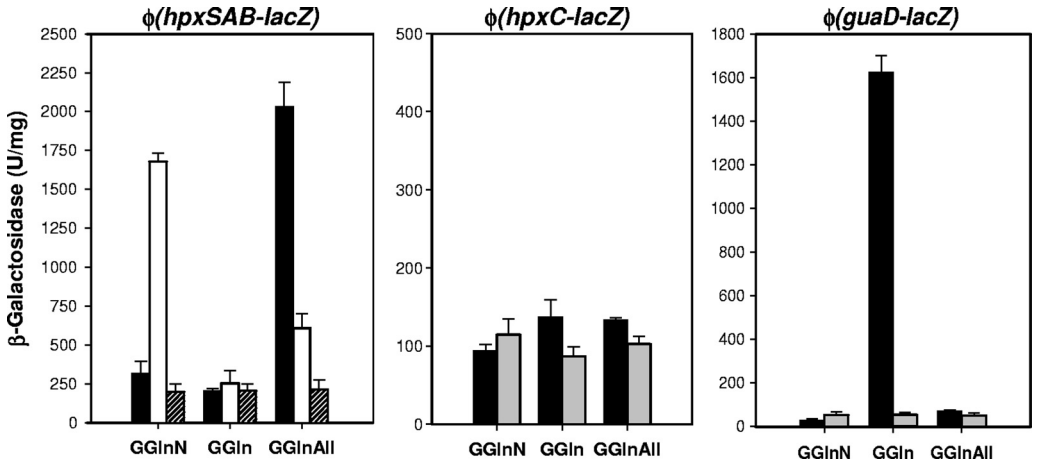

FIG. 3. Expression analysis of transcriptional fusions of the *hpxBASC-guaD* gene cluster in different genomic backgrounds and under different growth conditions. Cells of the parental strain KC2653 (black bars) and the derived *hpxS* (white bars), *nac* (dashed bars), or *ntrC* (gray bars) mutant strain bearing the promoter fusion Φ(*hpxSAB-lacZ*), Φ(*hpxC-lacZ*), or Φ(*guaD-lacZ*) were grown in the indicated culture media. GNGln is a nitrogen excess medium that contains 0.4% glucose and 0.2% each ammonium sulfate and Gln, GGln is a nitrogen-limiting medium that contains 0.4% glucose and 0.04% Gln, and GGlnAll is the nitrogen-limiting medium containing 0.05% allantoin. β-Galactosidase activity is expressed in units/mg. Error bars indicate standard deviations.

OHCU decarboxylases is *S*-allantoin, the presence of a gene encoding a putative racemase (*hpxA*) in the *hpxSAB* operon seems unnecessary. In fact, Pope et al. (28) showed that in *K. oxytoca* the *hpxA* function is dispensable for growth on racemic allantoin. HpxA may be important for efficient scavenging of external allantoin present at low concentration in the environment.

Effect of the nitrogen source on the expression of the *hpxSAB*, *hpxC*, and *guaD*. To study whether the expression of the gene cluster encompassing *hpxSAB*, *hpxC*, and *guaD* is regulated by nitrogen availability, the expression of the promoter fusions Φ(*hpxSAB-lacZ*), Φ(*hpxC-lacZ*), and Φ(*guaD-lacZ*) in the genetic background of strain KC2653 grown with different nitrogen sources was analyzed (Fig. 3, black bars). β-Galactosidase activity in glucose cultures with nitrogen excess (GNGln), nitrogen limitation (GGln), or nitrogen limitation in the presence of hypoxanthine (GGlnHx), guanosine (GGlnGns), or allantoin (GGlnAll) was measured.

The expression of Φ(*guaD-lacZ*) was repressed by nitrogen excess and induced approximately 100-fold under nitrogen-limiting conditions (GGln) (Fig. 3). Addition of hypoxanthine or guanosine to nitrogen-limiting cultures did not result in an increase of β-galactosidase activity with respect to the level for cultures grown in low-glutamine-concentration medium (GGln) (1,625 U/mg), indicating that *guaD* is mainly regulated by nitrogen limitation (not shown). Under these conditions, deamination of guanine would provide ammonia for growth. When allantoin was used as the nitrogen source or added to nitrogen-limiting cultures, repression of Φ(*guaD-lacZ*) was observed at levels close to those displayed by cells grown in high-ammonia medium (GNGln). In *Bacillus subtilis*, even though addition of allantoin to nitrogen-limiting cultures induces most of the genes of the purine catabolic pathway, the expression of those encoding the subunits of xanthine dehydrogenase is repressed (37). This repression may be important for reducing purine utilization as the nitrogen source when allantoin is present in the medium.

Regarding Φ(*hpxC-lacZ*), analysis of β-galactosidase activity showed that *hpxC*, which encodes the putative allantoin permease, is not regulated by nitrogen limitation. In this case, activity levels under limiting-nitrogen conditions (GGln) were scarcely 1.5-fold higher than those displayed by cells grown in high-ammonia medium (GNGln). Addition of allantoin to limiting-nitrogen cultures did not significantly modify β-galactosidase levels (Fig. 3).

Analysis of Φ(*hpxSAB-lacZ*) showed a different pattern of expression. This operon was slightly repressed under nitrogen-limiting conditions (GGln). Maximal induction was achieved by growth in GGln medium plus allantoin or with allantoin as the sole nitrogen source (Fig. 3). These results suggest additional control of Φ(*hpxSAB-lacZ*) by allantoin or derived metabolites. However, neither guanosine nor hypoxanthine, whose catabolism yields allantoin, nor allantoate, the next intermediate metabolite in the allantoin catabolic pathway, induced Φ(*hpxSAB-lacZ*) expression (β-galactosidase values were around 200 U/mg). The basal level of expression in guanosine or hypoxanthine medium may be sufficient to provide allantoinase activity to metabolize endogenous allantoin generated from uric acid oxidation and, hence, support growth on these compounds as the nitrogen source. However, in this case intracellular levels of allantoin or derived metabolites may not be high enough to trigger *hpxSAB* induction. We hypothesize that when allantoin is used as a nitrogen source, a higher intracellular level is achieved. In this case, allantoin itself or a derived metabolite not yet identified may act as the inducer molecule for *hpxSAB* expression.

We next examined whether this specific regulation is influenced by nitrogen availability. To this end, allantoin was added to high-ammonia medium (GNGlnAll). In these nitrogen excess conditions, allantoin did not induce *hpxSAB* expression (not shown). Thus, taken together, these results indicate that both signals, allantoin (or an allantoin-derived metabolite) and limiting nitrogen, are required for the transcriptional activation of Φ(*hpxSAB-lacZ*).

Expression of *hpxSAB*, *hpxC*, and *guaD* in *ntrC* and *nac* mutants. To further examine whether the regulation of *hpxSAB*, *hpxC*, and *guaD* transcriptional units is mediated by components of the Ntr system, the *nac* (strain KC5249) and *ntrC* (strain KC2738) mutations were introduced by P1 transduction into the genetic background of strain KC2653, bearing Φ(*hpxSAB-lacZ*), Φ(*hpxC-lacZ*), or Φ(*guaD-lacZ*). The expression of these transcriptional fusions in the derived mutants in cultures grown under different nitrogen conditions (GNGln, GGln, GGlnAll) was analyzed.

As expected, expression of Φ(*guaD-lacZ*) under nitrogen-limiting conditions was strongly reduced in the *ntrC* mutant (Fig. 3, gray bars). In this mutant, β-galactosidase levels were close to those obtained under nitrogen excess conditions. In contrast, no significant changes in the expression pattern of Φ(*guaD-lacZ*) were observed in the *nac* mutant background (not shown). These results are consistent with the presence of conserved NtrC binding sites upstream from the σ^{54} sequences in the *guaD* promoter (Fig. 2) and strongly support the involvement of NtrC in the regulation of this gene.

Expression of Φ(*hpxC-lacZ*) was not modified in the genomic background of the *ntrC* (Fig. 3) or *nac* (not shown) mutants. This is in accordance with the lack of regulation by nitrogen availability and reinforces the idea that transcription of this gene may be driven by σ^{70}-RNA polymerase.

Induction by allantoin of Φ(*hpxSAB-lacZ*) was abolished both in the *ntrC* (not shown) and the *nac* (Fig. 3, dashed bars) mutants. No significant differences in β-galactosidase levels were observed in cultures of these mutants performed under high- or limiting-nitrogen conditions (Fig. 3). Since *hpxSAB* is transcribed by a σ^{70}-dependent RNA polymerase, the NtrC effect must be indirect, through the action of NAC. In fact, a recent report on chromatin immunoprecipitation analysis revealed the 5′ upstream region of *hpxSAB* as a putative target of NAC (13). These results strongly suggest that NAC is one of the regulators required for full induction of Φ(*hpxSAB-lacZ*) by allantoin.

Role of HpxS in the regulation of the *hpxBASC-guaD* gene cluster. As described for *K. oxytoca* (28), the *hpxS*-encoded protein is a member of the large GntR family of transcriptional regulators which is formed by four subfamilies. *In silico* analysis indicated that HpxS belongs to the FadR subfamily. The regulators belonging to this subfamily share a similar amino-terminal helix-turn-helix domain, which recognizes a consensus sequence, 5′-NNNTN**GT**ANT**AC**NANNN-3′ (conserved nucleotides defining the consensus are in bold). In contrast, these regulators display high heterogeneity in the C-terminal effector and oligomerization domain (31).

To evaluate the role of HpxS as a transcriptional regulator of this gene cluster, a knockout mutant in which the gene encoding HpxS was disrupted by a Km cassette (strain KB17K) was generated. Phenotypic analysis of this mutant revealed that HpxS deficiency did not abolish allantoin utilization as a nitrogen source. To confirm its role as a regulator, the expression of Φ(*hpxSAB-lacZ*), Φ(*hpxC-lacZ*), and Φ(*guaD-lacZ*) in the *hpxS* mutant grown under different nitrogen conditions was analyzed (Fig. 3, white bars). Induction of Φ(*hpxSAB-lacZ*) by allantoin was reduced 3-fold in this mutant, suggesting that the function of HpxS in the presence of allantoin is the transcriptional activation of the *hpxSAB* operon. In a high-ammonia concentration (GNGln), β-galactosidase values were 4-fold higher than that of the parental strain (Fig. 3), which suggests that HpxS could act as a repressor in the absence of allantoin, whereas in a low-ammonia concentration (GGln), no increase in β-galactosidase activity was observed (Fig. 3). These results suggest that, in the absence of HpxS, NAC can act as a repressor of *hpxSAB* transcription. The intermediate levels of β-galactosidase observed in the *hpxS* mutant grown in low-ammonia medium plus allantoin (GGlnAll) may be attributed to parallel intermediate NAC intracellular levels under this condition.

Regarding Φ(*hpxC-lacZ*) and Φ(*guaD-lacZ*), the results showed no significant changes in their expression pattern in the genetic background of the *hpxS* mutant with respect to the levels for the parental strain KC2653 (not shown), indicating that HpxS is not involved in the transcriptional control of *hpxC* and *guaD*.

This set of results indicates that in the *hpxBASC-guaD* gene cluster, only the *hpxSAB* operon is regulated by HpxS. This protein may have a dual role, acting as a repressor in the absence of allantoin and as an activator in its presence. However, full activation of *hpxSAB* by allantoin also requires the participation of NAC.

Analysis of binding of HpxS to promoter regions of the *hpxBASC-guaD* gene cluster. Binding of HpxS to the intergenic region of *hpxSAB-hpxC* was studied by electrophoretic mobility shift assays (EMSA). The interactions with the complete *hpxSAB-hpxC* intergenic region were assessed using HpxS protein, purified as described in Materials and Methods, and probe P360 (Fig. 4B, left panel). The results showed binding of HpxS to this probe. This is consistent with the proposed role for HpxS in the regulation of *hpxSAB*. Binding experiments were also performed in the presence of allantoin and other metabolic intermediates of the purine degradation pathway, such as guanine or uric acid (upstream pathway metabolites) and allantoate, ureidoglycolate, or oxamate (downstream pathway metabolites). None of these compounds abolished binding of HpxS to probe P360 (not shown). Only allantoin seemed to modify the pattern of complexes formed, diminishing the amount of the less retarded complex (Fig. 4B, left panel).

Regarding *guaD*, no retarded complexes were observed in EMSA performed with HpxS and a probe encompassing the 5′ upstream region of this gene (positions −156 to +83) (not shown). This is consistent with the results obtained in the expression analysis of *guaD* in the genetic background of an *hpxS* mutant and clearly rules out a direct role for HpxS in *guaD* control.

To locate the HpxS binding site more precisely in the *hpxSAB-hpxC* intergenic region, eight additional fragments, corresponding to deletions of this intergenic region, were tested as probes in subsequent electrophoretic mobility shift experiments (Fig. 4A and B). HpxS bound to P1, P2, P3, P5, and P6 but not to P4, P7, or P8. Binding of HpxS to the nonoverlapping fragments P3 and P5 (Fig. 4B) indicated the presence of two binding sites for this protein in the *hpxS* promoter region. An *in silico* analysis of this region allowed us to identify the palindromic sequences (5′-TTTAT**GT**AT**AC**G<u>A</u>TCT-3′ and 5′-ATC<u>TT</u>**GT**ATA**AC**A<u>A</u>AAA-3′) almost matching the consensus sequence for the GntR regulators, although in both cases only two positions are present between the conserved GT and AC (consensus nucleotides are in bold,

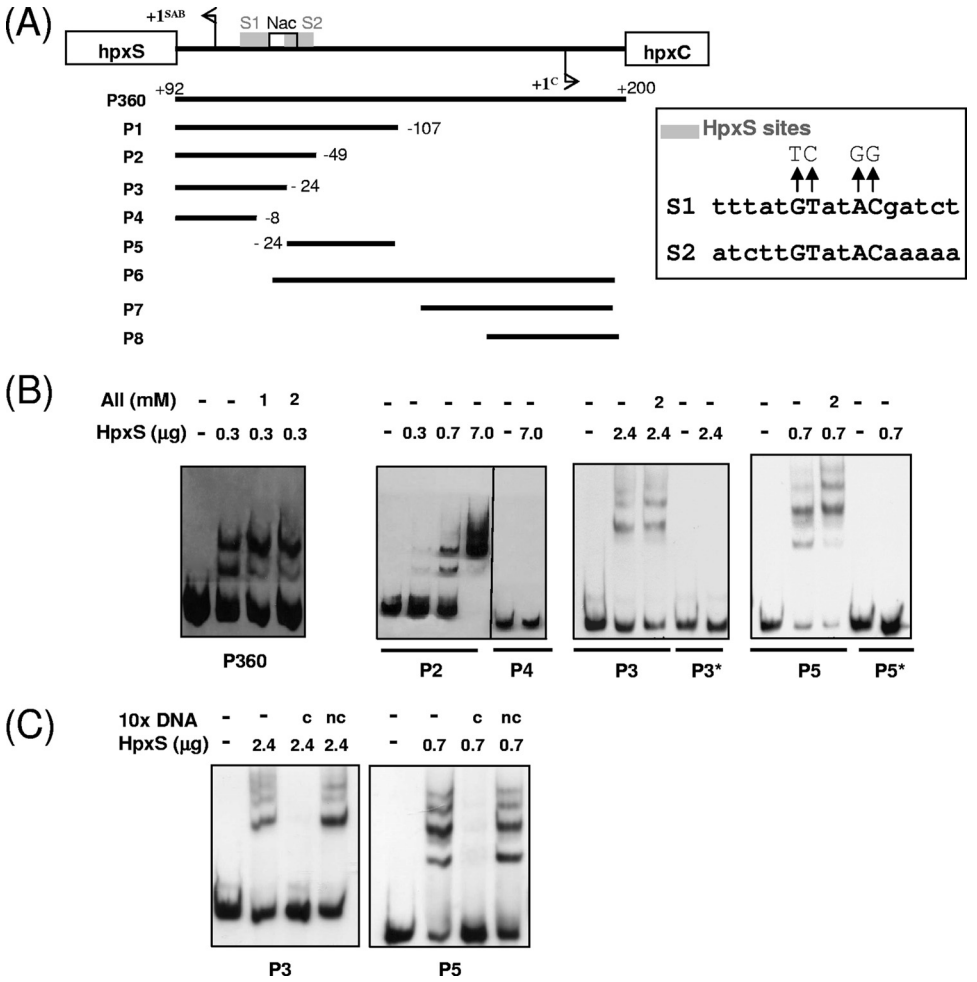

FIG. 4. Binding of HpxS to promoter fragments of the *hpxSAB* operon. (A) Diagram of the *hpxS-hpxC* intergenic region showing the transcription start site for each gene. The promoter fragments used as probes and their end terminus positions with respect to position +1 of *hpxS* are shown below. Position +200 in P360 is given according to position +1 of *hpxC*. Mutations introduced by site-directed mutagenesis in the HpxS binding sites S1 and S2 (gray boxes) are shown above the corresponding wild-type sequences. The Nac binding site is indicated by a white box. (B) EMSA performed with recombinant HpxS and the indicated probes. The digoxigenin-labeled probes covering different parts of the *hpxS-hpxC* intergenic region were added to binding mixtures containing HpxS in the absence or presence of allantoin at the indicated concentrations. Probes P3* and P5* contained the indicated mutations in the HpxS S1 and S2 binding sites, respectively. All mixtures contained 500-fold molar excesses of poly(dI-dC). Reaction mixtures were incubated at 30°C for 15 min and directly subjected to PAGE. (C) EMSA of the HpxS-S1 and HpxS-S2 complexes in the presence of competing or noncompeting DNA. As competing DNA (c), a 10-fold excess of the same nonlabeled probe (P3 or P5) was used. In both cases, nonlabeled probe P4 was added to binding mixtures as noncompeting DNA (nc).

and other matching nucleotides are underlined) (Fig. 2). One binding site (site S1) was located between positions −4 and −19 with respect to the *hpxS* transcriptional start site and the other (site S2) between positions −26 and −41 (Fig. 2). Thus, these tandem S1 and S2 sites are orientated in the same helical phase. Specificity of binding of HpxS to these sites was assessed in control experiments performed with nonlabeled competing DNA (Fig. 4C). Notice that approximately 3-fold-larger amounts of HpxS were used in EMSA performed with probe P3 with respect to probe P5 (Fig. 4B and C), suggesting that this protein may display greater affinity for S2 than for S1. Addition of allantoin to binding mixtures did not modify the pattern of HpxS complexes with site S1 (probe P3) but significantly reduced the amount of the less retarded complex in favor of the more retarded one with site S2 (probe P5) (Fig. 4B). This suggests that allantoin may induce a conformational change in HpxS bound to S2 that modifies its oligomerization state, thus reinforcing the idea that allantoin can act as an effector molecule of HpxS function.

To confirm that HpxS binds to these sequences, site-directed mutagenesis of the two conserved nucleotides in each half-site of both palindromes was performed (Fig. 4A). Gel shift experiments showed that these mutations abolished HpxS binding (Fig. 4B).

Other regulators belonging to the FadR subfamily bind to more than one operator site in the target promoter and have been described to have a dual role. For instance, in *E. coli*, LldR acts as a repressor of *lldPRD* expression in the absence of L-lactate, but in the presence of L-lactate, LldR acts as an activator. In this model, the regulatory protein binds to two operator sequences in the *lldPRD* operon, leading to DNA looping and the repression of transcription. Binding of the

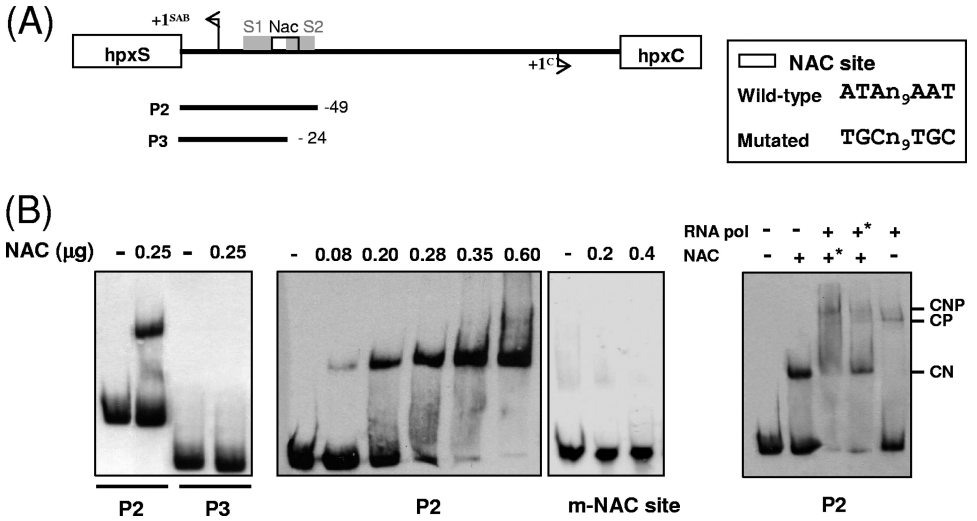

FIG. 5. Binding of NAC to promoter fragments of the *hpxSAB* operon. (A) Diagram of the *hpxS-hpxC* intergenic region showing the transcription start site for each gene. The promoter fragments used as probes and their end terminus positions with respect to position +1 of *hpxS* are shown below. Mutations introduced by site-directed mutagenesis in the NAC binding site (white box) are shown above the corresponding wild-type sequences. (B) EMSA performed with recombinant NAC. The indicated digoxigenin-labeled probes were added to binding mixtures containing the indicated amounts of NAC. Probe m-NAC site corresponds to the mutated NAC binding site probe. Binding of NAC in the presence of RNA polymerase is shown in the right panel. In this experiment, NAC was added at 0.25 μg and RNA polymerase at 0.28 μg. Where both proteins were present, the asterisk indicates the first protein added to the binding mixtures. CN, retarded complex with NAC; CP, retarded complex with RNA polymerase; and CNP, retarded complex with both proteins. All mixtures contained 500-fold molar excesses of poly(dI-dC). Reaction mixtures were incubated at 20°C for 15 min and directly subjected to PAGE.

inducer L-lactate to LldR promotes a conformational change that disrupts the DNA loop, allowing the formation of the transcription open complex (1). Concerning HpxS, the short distance between the two HpxS binding sites, S1 and S2, does not allow DNA looping. Since both HpxS sites are orientated in the same helical phase, side-by-side interaction of HpxS molecules bound to tandem S1 and S2 sites can mediate *hpxSAB* repression. The activator role of HpxS in the presence of allantoin may depend on conformational changes induced by this effector molecule. However, allantoin itself is not sufficient to relieve *hpxSAB* repression. The results of the transcriptional fusion analysis indicated that NAC is required for activation of *hpxSAB* transcription.

Analysis of binding of NAC to the *hpxSAB-hpxC* intergenic region. Our results pointed to NAC as a regulator of *hpxSAB* expression. In addition, as stated above, the *hpxSAB-hpxC* intergenic region has recently been identified among the promoter sequences coimmunoprecipitated with NAC in *K. pneumoniae* (13).

Binding of NAC to the *hpxSAB-hpxC* intergenic region was analyzed by EMSA with purified NAC protein and probes encompassing different sequences of this region (Fig. 5). Purified NAC bound to P1 and P2 but not to P3, P4, and P5.

Regarding *guaD*, as expected for a σ^{54}-dependent gene, no retarded complexes were observed in EMSA performed with NAC and a probe encompassing the 5′ upstream region of *guaD* (positions −156 to +83) (not shown).

To further characterize binding of NAC to the *hpxSAB* promoter, different amounts of NAC were used in gel shift experiments with probe P2 (Fig. 5B). Binding of NAC to this probe was observed at concentrations similar to those described for other promoters, which are in the range of 1 to 5 pmol (33). An *in silico* analysis of this region allowed us to identify a conserved NAC binding site (5′-ATAN$_9$AAT-3′) between positions −20 and −34 with respect to the transcriptional start site of *hpxSAB* (Fig. 2). Indeed, site-directed mutagenesis of conserved residues in this palindrome (5′-TGCN$_9$TGC-3′) abolished NAC binding (Fig. 5B).

Since this NAC site partially overlaps the −35 σ^{70} recognition sequence for *hpxSAB* transcription, EMSA were performed to analyze the effect of NAC on RNA polymerase binding. To this end, binding of *E. coli* K-12 RNA polymerase (Sigma-Aldrich, Germany) to probe P2 was analyzed in the absence or presence of NAC (Fig. 5B). Preincubation of probe P2 with NAC before the addition of RNA polymerase resulted in the formation of a new retarded complex (CNP) of higher molecular mass than the complex obtained with RNA polymerase alone (CP) or NAC alone (CN). These results indicated that both proteins bind to this probe simultaneously. In addition, preincubation with NAC also increased the intensity of the band corresponding to the CNP complex in comparison with the level for binding reactions in which RNA polymerase was added before NAC. These results indicated that *in vitro* NAC has a positive effect on binding of RNA polymerase to the *hpxSAB* promoter. However, transcriptional fusion analysis showed that in the absence of HpxS (*hpxS* mutant), NAC, expressed under limiting-nitrogen conditions (GGln), represses *hpxSAB* transcription (Fig. 3, white bars).

Taken together, these results suggest that the activator function of NAC *in vivo* depends on its interplay with HpxS in the presence of allantoin. In the *hpxSAB* promoter, the NAC binding site (centered at position −27) is located between S1 (centered at position −12) and S2 (centered at position −33) and partially overlaps S2 (Fig. 2). As NAC will bind opposite to

HpxS, it is tempting to speculate that NAC may contact HpxS bound to S2, leading to the disruption of the interactions between the HpxS molecules bound to S1 and S2. Although NAC can help the recruitment of RNA polymerase to the *hpxSAB* promoter, transcriptional activation of this operon requires the presence of allantoin. This effector molecule binds to HpxS, probably to its C-terminal domain as described for other members of the GntR family, and would promote a conformational change that modifies HpxS function. In this context, it is conceivable that the conformational change induced in HpxS bound to S2 may modify NAC conformation and its interaction with RNA polymerase, leading to the formation of a transcription open complex and the activation of *hpxSAB* transcription. More work would be needed to define the interactions of NAC with HpxS.

Thus, the presence in the *hpxSAB* promoter of two HpxS binding sites (S1 and S2) and a NAC binding site located between S1 and S2 and partially overlapping S2 led us to propose that the activity of this promoter is modulated depending on the differential binding of HpxS and NAC to these *cis*-acting elements in response to different metabolic conditions (allantoin and nitrogen availability).

ACKNOWLEDGMENTS

This research was supported by grants BFU 2007-63090/BMC and BFU2010-22260-C02-01 from the Ministerio de Educación y Ciencia, Spain, to L.B. K.G. received a predoctoral fellowship from the Generalitat de Catalunya, Spain.

We thank Robert A. Bender for providing strain EB4335 and for critical reading of the manuscript.

REFERENCES

1. **Aguilera, L., et al.** 2008. Dual role of LldR in regulation of *lldPRD* operon, involved in L-lactate metabolism in *Escherichia coli*. J. Bacteriol. **190:**2997–3005.
2. **Baldauf, S. L., M. A. Cardani, and R. A. Bender.** 1988. Regulation of the galactose-inducible *lac* operon and the histidine utilization operons in *pts* mutants of *Klebsiella aerogenes*. J. Bacteriol. **170:**5588–5593.
3. **Batie, C. J., D. P. Ballou, and C. C. Correll.** 1992. Phthalate dioxygenase reductase and related flavin-iron-sulfur containing electron transferases, p. 543–556. *In* F. Müller (ed.), Chemistry and biochemistry of flavoenzymes. CRC Press, Boca Raton, FL.
4. **Bender, R. A., et al.** 1977. Biochemical parameters of glutamine synthetase from *Klebsiella aerogenes*. J. Bacteriol. **129:**1001–1009.
5. **Bender, R. A., P. M. Snyder, R. Bueno, M. Quinto, and B. Magasanik.** 1983. Nitrogen regulation system of *Klebsiella aerogenes*: the *nac* gene. J. Bacteriol. **156:**444–446.
6. **Bender, R. A., and B. Friederich.** 1990. Regulation of assimilatory nitrate reductase formation in *Klebsiella aerogenes* W70. J. Bacteriol. **172:**7256–7259.
7. **Bertani, G.** 2004. Lysogeny at mid-twentieth century: P1, P2, and other experimental systems. J. Bacteriol. **186:**595–600.
8. **Cusa, E., N. Obradors, L. Baldoma, J. Badia, and J. Aguilar.** 1999. Genetic analysis of a chromosomal region containing genes required for assimilation of allantoin nitrogen and linked glyoxylate metabolism in *Escherichia coli*. J. Bacteriol. **181:**7479–7748.
9. **Datsenko, K. A., and B. L. Wanner.** 2000. One-step inactivation of chromosomal genes in *Escherichia coli* K-12 using PCR products. Proc. Natl. Acad. Sci. U. S. A. **97:**6640–6645.
10. **de la Riva, L., J. Badia, J. Aguilar, and L. Baldoma.** 2008. The *hpx* genetic system for hypoxanthine assimilation as a nitrogen source in *Klebsiella pneumoniae*: gene organization and transcriptional regulation. J. Bacteriol. **190:**7892–7903.
11. **Feng, J., T. J. Goss, R. A. Bender, and A. J. Ninfa.** 1995. Repression of the *Klebsiella aerogenes nac* promoter. J. Bacteriol. **177:**5535–5538.
12. **Fernández, J. R., B. Byrne, and B. L. Firestein.** 2009. Phylogenetic analysis and molecular evolution of guanine deaminases: from guanine to dendrites. J. Mol. Evol. **68:**227–235.
13. **Frisch, R. L., and R. A. Bender.** 2010. Expanded role for the nitrogen assimilation control protein (NAC) in the response of *Klebsiella pneumoniae* to nitrogen stress. J. Bacteriol. **192:**4812–4820.
14. **Frisch, R. L., and R. A. Bender.** 2010. Properties of the NAC-binding site within the *ureD* promoter of *Klebsiella pneumoniae*. J. Bacteriol. **192:**4821–4826.
15. **Goldberg, R. B., R. A. Bender, and S. L. Streicher.** 1974. Direct selection for P1-sensitive mutants of enteric bacteria. J. Bacteriol. **118:**810–814.
16. **Hidalgo, E., and B. Demple.** 1997. Spacing of promoter elements regulates the basal expression of the *soxS* gene and converts SoxR from a transcriptional activator into a repressor. EMBO J. **16:**1056–1065.
17. **Huerta, A. M., M. P. Francino, E. Morett, and J. Collado-Vides.** 2006. Selection for unequal densities of σ^{70} promoter-like signals in different regions of large bacterial genomes. PLoS Genet. **2:**1740–1749.
18. **Janes, B. K., and R. A. Bender.** 1998. Alanine catabolism in *Klebsiella aerogenes*: molecular characterization of the *dadAB* operon and its regulation by the nitrogen assimilation control protein. J. Bacteriol. **180:**563–570.
19. **Laemmli, U. K.** 1970. Cleavage of structural proteins during the assembly of the head of bacteriphage T4. Nature **227:**680–685.
20. **LaPointe, G., S. Viau, D. LeBlanc, N. Robert, and A. Morin.** 1994. Cloning, sequencing, and expression in *Escherichia coli* of the D-hydantoinase gene from *Pseudomonas putida* and distribution of homologous genes in other microorganisms. Appl. Environ. Microbiol. **60:**888–895.
21. **Lee, K. W., and A. H. Roush.** 1964. Allantoinase assays and their application to yeast and soybean allantoinases. Arch. Biochem. Biophys. **108:**460–467.
22. **Liu, Q., and R. A. Bender.** 2007. Complex regulation of urease formation from the two promoters of the *ure* operon of *Klebsiella pneumoniae*. J. Bacteriol. **189:**7593–7599.
23. **Lowry, O. H., N. J. Rosebrough, A. L. Farr, and R. J. Randall.** 1951. Protein measurement with the Folin Phenol reagent. J. Biol. Chem. **193:**265–273.
24. **Macaluso, A., E. A. Best, and R. A. Bender.** 1990. Role of *nac* gene product in the nitrogen regulation of some NTR-regulated operons of *Klebsiella aerogenes*. J. Bacteriol. **172:**7249–7255.
25. **MacPhee, D. G., I. W. Sutherland, and J. F. Wilkinson.** 1969. Transduction in *Klebsiella*. Nature **221:**475–476.
26. **Miller, J. H.** 1992. A short course in bacterial genetics. Cold Spring Harbor Laboratory Press, Cold Spring Harbor, NY.
27. **O'Leary, S. E., K. A. Hicks, S. E. Ealick, and T. P. Begley.** 2009. Biochemical characterization of the HpxO enzyme from Klebsiella pneumoniae, a novel FAD-dependent urate oxidase. Biochemistry **48:**3033–3045.
28. **Pope, S. C., L. L. Chen, and V. Stewart.** 2009. Purine utilization by *Klebsiella oxytoca* M5a1: genes for ring-oxidizing and -opening enzymes. J. Bacteriol. **191:**1006–1017.
29. **Ramazzina, I., et al.** 2008. Logical identification of an allantoinase analog (*puuE*) recruited from polysaccharide deacetylases. J. Biol. Chem. **283:**23295–23304.
30. **Reitzer, L.** 2003. Nitrogen assimilation and global regulation in *Escherichia coli*. Annu. Rev. Microbiol. **57:**155–176.
31. **Rigali, S., A. Derouaux, F. Giannotta, and J. Dusart.** 2002. Subdivision of the helix-turn-helix GntR family of bacterial regulators in the FadR, HutC, MocR, and YtrA subfamilies. J. Biol. Chem. **277:**12507–12515.
32. **Rintoul, M. R., et al.** 2002. Regulation of the *Escherichia coli* allantoin regulon: coordinated function of the repressor AllR and activator AllS. J. Mol. Biol. **324:**599–610.
33. **Rosario, C. J., and R. A. Bender.** 2005. Importance of a tetramer formation by the nitrogen assimilation control protein for strong repression of glutamate dehydrogenase formation in *Klebsiella pneumoniae*. J. Bacteriol. **187:**8291–8299.
34. **Rouf, M. A., and R. F. Lomprey.** 1968. Degradation of uric acid by certain aerobic bacteria. J. Bacteriol. **96:**617–622.
35. **Saint-Marc, C., et al.** 2009. Phenotypic consequences of purine nucleotide imbalance in *Saccharomyces cerevisiae*. Genetics **183:**529–538.
36. **Sambrook, J., and D. W. Russell.** 2001. Molecular cloning: a laboratory manual. Cold Spring Harbor Laboratory, Cold Spring Harbor, NY.
37. **Schultz, A. C., P. Nygaard, and H. H. Saxild.** 2001. Functional analysis of 14 genes that constitute the purine catabolic pathway in *Bacillus subtilis* and evidence for a novel regulon controlled by the PucR transcription activator. J. Bacteriol. **183:**3293–3302.
38. **Schwacha, A., and R. A. Bender.** 1993. The product of the *Klebsiella aerogenes nac* (nitrogen assimilation control) gene is sufficient for activation of the *hut* operons and repression of the *gdh* operon. J. Bacteriol. **175:**2116–2124.
39. **Simons, R. W., and F. Houmanand.** 1987. Improved single and multicopy lac-based cloning vectors for protein and operon fusions. Gene **53:**85–96.
40. **Skorupski, K., and R. K. Taylor.** 1996. Positive selection vectors for allelic exchange. Gene **169:**47–52.
41. **Smith, G. R., S. H. Yeheskel, and B. Magasanik.** 1971. Genetic and metabolic control of enzymes responsible for histidine degradation in *Salmonella typhimurium*. J. Biol. Chem. **246:**3320–3329.
42. **Vogels, G. D., and C. Van der Drift.** 1976. Degradation of purines and pyrimidines by microorganisms. Bacteriol. Rev. **40:**403–468.
43. **Xi, H., B. L. Schneider, and L. Reitzer.** 2000. Purine catabolism in *Escherichia coli* and function of xanthine dehydrogenase in purine salvage. J. Bacteriol. **182:**5332–5341.
44. **Yoo, H. S., F. S. Genbauffe, and T. G. Cooper.** 1985. Identification of the ureidoglycolate hydrolase gene in the *DAL* gene cluster of *Saccharomyces cerevisiae*. Mol. Cell. Biol. **5:**2279–2288.